ADVANCES IN ATMOSPHERIC SCIENCES, VOL. 31, NOVEMBER 2014, 1395–1406

A Study on the Physical Processes of the Formation of the ENSO Cycle

ZONG Haifeng*

International Center for Climate and Environment Sciences, Institute of Atmospheric Physics, Chinese Academy of Sciences, Beijing 100029

(Received 18 November 2013; revised 5 March 2014; accepted 11 April 2014)

ABSTRACT

The physical processes involved in the formation of the ENSO cycle, as well as the possible roles of the Hadley circulation (HC), Walker circulation (WC), and the propagating waves of the Southern Oscillation/Northern Oscillation (SO/NO) in its formation, were studied using composite and regression methods. The analysis showed that the convection and heat release triggered by ENSO in the central-eastern equatorial Pacific are the primary drivers for the 3–5 year cycle of the HC, WC and the meridional/zonal circulation. The HC plays a key role in the influence of ENSO on the circulation outside the tropics through angular momentum transportation. Meanwhile, the feedback effects of the anomalous circulation in the mid-high latitudes on ENSO are accomplished by the propagating waves of SO/NO associated with the evolutions of HC and WC. These propagating waves are the main agents of the connections among the meridional/zonal circulation outside the tropics, the Asian/Australian monsoon, the anomalous easterly/westerly winds over the tropical Pacific, and ENSO events. It was found that the 3–5 year cycle of the meridional/zonal circulation forced by ENSO is quite different from the several-week variation of the circulation index triggered by the inner dynamic processes of the atmosphere. The former occurs at the global scale with a definite flow pattern, while the latter occurs only in a wide area without a definite flow pattern. Finally, a physical model for the formation of the ENSO cycle composed of two fundamental processes at the basin and global scale, respectively, is proposed.

Key words: ENSO cycle, meridional/zonal circulation, Hadley circulation, propagating waves, Southern Oscillation/Northern Oscillation

Citation: Zong, H. F., 2014: A study on the physical processes of the formation of the ENSO cycle. *Adv. Atmos. Sci.*, **31**(6), 1395–1406, doi: 10.1007/s00376-014-3224-2.

1. Introduction

Since Bjerknes (1966) revealed the close connection between El Niño and Southern Oscillation (SO), ENSO has been a hot topic in meteorology and oceanography. Today, ENSO forcing is regarded as the chief factor leading to global climate variation so far, and more climate simulations and predictions associated with ENSO, compared to other forcings, are performed using general circulation models (GCMs). However, simulation and prediction of the climate, especially precipitation, are still far from satisfactory due to the limits of GCMs, which partly result from our incomplete knowledge about the feedbacks between the atmosphere and ENSO.

To improve the simulation and prediction of ENSO, as well as the climate, theories regarding the formation of the ENSO cycle have been proposed from the perspective of oceanic dynamics, such as equatorial ocean wave action (McCreary and Julian, 1983; Schopf and Suarez, 1988; Suarez and Schopf, 1988), the instability of air–sea interaction (Philander et al., 1984; Cane and Zebiak, 1985; Chao and Zhang, 1988; Zhang and Chao, 1993), and the delayed-oscillator mechanism (Hirst, 1988; Battisti and Hirst, 1989). These theories have improved our understanding of the effects of equatorial ocean waves and unstable air–sea coupling on the ENSO cycle. Regarding observational studies on the formation of ENSO, Bjerknes (1966) first pointed out that the warming (cooling) in the central-eastern equatorial Pacific results from the weakened (strengthened) upwelling of low-level cold water caused by the weakened (strengthened) trade winds in the southern Pacific. He also noted that the weakening (strengthening) of southeast trade winds is closely related to SO variation. Chen (1982) studied the interaction between subtropical anticyclones in the northern Pacific and the SST of the eastern equatorial Pacific and put forward a conceptual model for the interaction process. Rasmusson and Carpenter (1982) put forward a composite model regarding the evolution of tropical winds and SST in different phases of an ENSO event. These two aspects of study have shown the effects on the ENSO cycle of equatorial ocean waves, including the instability of air–sea coupling, and the trade winds over the Pacific, but the linkages between some of the phenomena have not been further discussed.

* Corresponding author: ZONG Haifeng
Email: zhf@mail.iap.ac.cn

Since the 1982/83 El Niño event, more attention has been paid to the SST anomalies of the western Pacific warm pool and the effects of zonal wind anomalies there. Keen (1982) and Nitta (1989) pointed out that the development of the cross-equatorial tropical cyclone pair (CECP) and a burst of westerly wind anomalies in the western tropical Pacific, play an important role in the enhancement and eastward expansion of positive SST anomalies from the western Pacific warm pool. Some studies have found that such westerly wind anomalies are an essential condition for the development of an El Niño event (Wyrtki, 1975; Fu and Huang, 1996; Zhang et al., 2000; Wang et al., 2004; Li et al., 2010), and their appearances are closely related to the East Asia winter monsoon (EAWM) (Li, 1988) and the equatorward propagations of the extratropical westerly wind anomalies (Huang and Fu, 1996). Meanwhile, Chen and Fan (1993) and Wu and Chen (1995) noticed that the appearances of westerly wind caused by the EAWM are more frequent than ENSO events. They suggested that only those westerly winds bursting with an eastward propagation of a CECP at their flanks can lead to the occurrence of an El Niño event. The common effects of atmospheric circulation anomalies in the mid-high latitudes and propagating waves of SO and Northern Oscillation (NO) on the ENSO cycle were first highlighted in their studies. However, how the circulation in the mid-high latitudes and ENSO interact and how the propagating waves of SO/NO form were still unsolved in these works.

As a result of improving knowledge with respect to the dynamics and modeling of ENSO, prediction of ENSO has become routine practice in many countries. However, the prediction skill of most current ENSO models decreases sharply as the lead time increases, and becomes completely unskillful at a lead time of around nine months (Chen and Cane, 2008). It is possible, by introducing an embedded entrainment temperature parameterization (Zhu et al., 2013) or a nonlinear model using a neural network (Wu et al., 2006), for Niño region SST–anomalies to be forecasted quantitatively by up to 15 months in advance, but the boreal spring predictability barrier still remains unsolved (Zhu et al., 2013).

Further understanding of the physical processes of the ENSO cycle may be helpful in finding solutions to the aforementioned problems; in particular, through analysis of the physical processes independently of GCMs. In this context, the aim of the present study is to propose a new physical model of the formation of the ENSO cycle that consists of contributions from the air–sea interactions in the tropics, the circulation in the mid-high latitudes, the Asian and Australian monsoons, and equatorial Pacific wind and SST.

2. Data and methods

The monthly reanalysis datasets of the National Centers for Environmental Prediction and the National Center for Atmospheric Research (NCEP/NCAR) (Kalnay et al., 1996) (including geopotential height, horizontal and vertical velocity, 1000–500 hPa thickness, latent heat flux, and surface upward longwave radiation flux) and the precipitation reconstruction dataset of the National Oceanic and Atmospheric Administration (NOAA) are used in the present study.

Version 3b of the Extended Reconstructed Sea Surface Temperature dataset (Smith et al., 2008) developed at the NOAA, and the monthly Niño3.4 SST data obtained from the NOAA's Climate Prediction Center (CPC), are also used.

Twenty-five strong ENSO winters used in this paper were selected from the ENSO episodes defined at the CPC, including 14 strong El Niño winters (1957/58, 1963/64, 1965/66, 1968/69, 1972/73, 1982/83, 1986/87, 1987/88, 1991/92, 1994/95, 1997/98, 2002/03, 2006/07, 2009/10) and 11 strong La Niña winters (1955/56, 1970/71, 1973/74, 1975/76, 1984/85, 1988/89, 1998/99, 1999/2000, 2007/08, 2010/11, 2011/12).

All the above data cover the period 1951–2012, and the climate means were calculated as the average of the period 1981–2010.

Composite and lagging regression methods are used to obtain the main features of the circulation and SST anomalies related to ENSO.

3. Variation of circulation related to ENSO

Bjerknes (1966) noticed early on that the westerly winds in the midlatitudes of the North Pacific become strengthened (weakened) during winters with warm (cold) SST in the tropical eastern Pacific. He attributed such variations of westerly winds in the midlatitudes of the North Pacific to the adjustments of the Hadley circulation (HC) and angular momentum transportation triggered by the tropical eastern Pacific SST. Since then, more recent studies have noted the impacts of ENSO are not just confined to the tropical Pacific, but extend globally (Yun et al., 2008; Zong et al., 2008; Wu et al., 2012), usually peaking in boreal winter (Tang, 2002; Xie et al., 2003). In this section, to better understand the main features of global circulation anomalies forced by ENSO, the spatiotemporal distributions of the global circulation anomalies during the peak phase (winter, December to February) of ENSO are further examined.

3.1. *Lower-troposphere thickness*

Figure 1 is the composite of normalized 1000–500 hPa thickness anomalies, surface upward longwave radiation flux (SULWRF) anomalies, precipitation anomalies, and SST anomalies during the peak phase of ENSO. During the peak phase of El Niño, significant positive 1000–500 hPa thickness anomalies (Fig. 1a) cover nearly the whole of the tropical regions, except the western tropical Pacific, with central values exceeding 0.9 and 0.3 standard deviations over the central-eastern equatorial Pacific and the tropical Indian Ocean, respectively. It shows that the thickness increases remarkably in the tropics, especially the central-eastern equatorial Pacific and tropical Indian Ocean. At the same time, the thickness increases along the Asian coast and over northern America but decreases over the northeastern Pacific and the southern

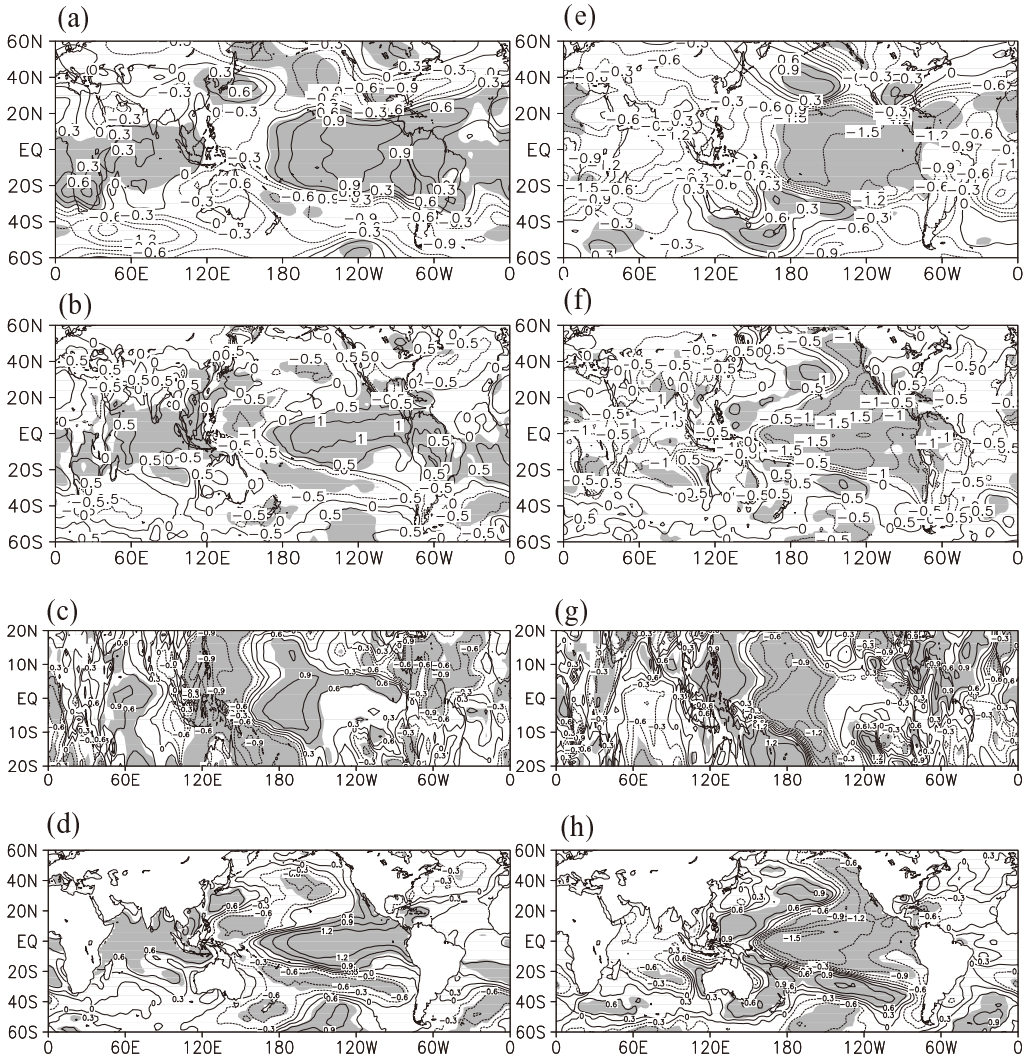

Fig. 1. Composite of normalized (a) 1000–500 hPa thickness anomalies, (b) SULWRF anomalies, (c) precipitation anomalies, and (d) SST anomalies during the peak phase of El Niño. Panels (e–h) are the same as (a–d), except for during the peak phase of La Niña. Anomalies at the 0.05 significance level are shaded.

flank of North America; while in the Southern hemisphere, the thickness increases along the low pressure belt around the Antarctic Pole, with three anomaly centers near the vicinity of the three mean troughs of the Southern Hemisphere, but decreases in the subtropics near the South Indian and Pacific oceans. Such a distribution indicates that the East Asia major trough withers and retreats northward, the Aleutian low extends southeastward, and the North American major trough is deepening. In addition, the mean troughs of the Southern Hemisphere are weakening, presenting a feature of more zonally-oriented circulation in the mid-high latitudes of both hemispheres, especially over the mid-high latitudes of the Asia–Pacific area. Moreover, such a distribution is also indicative of the prevalence of the North Pacific Oscillation (NPO), the Pacific/North America (PNA) and the Arctic Oscillation (AAO) flow patterns. Meanwhile, for La Niña, the distribution of the lower-troposphere thickness anomalies (Fig. 1e) is generally opposite to that of El Niño, showing a feature with more meridional-oriented circulation patterns characterized by a strong East Asia trough, negative NPO and PNA flow patterns in the mid-high latitudes of the Northern Hemisphere, and a negative AAO flow pattern in the mid-high latitudes of the Southern Hemisphere.

Comparing Figs. 1a–c with Figs. 1e–g, it can be seen that the positive (negative) thickness anomalies are located over the area where the SULWRF and precipitation strengthens (weakens). As is well known, the lower-troposphere thickness corresponds to the mean lower-troposphere temperature, which is tightly related to heating from surface and latent heat released by convection. Therefore, the profiles of Figs. 1a–c and Figs. 1e–g suggest that the lower-tropospheric thermal (circulation) variation is triggered or partly triggered by the adjustments of SULWRF and convection. Because the SULWRF is dominated by the surface temperature, and the tropical precipitation is also tightly related to water temperature (Bjerknes, 1969), the distributions of SULWRF anomalies in Figs. 1b and f are very similar to those of SST anomalies during the peak phase of El Niño (Fig. 1d) and La Niña

(Fig. 1h), respectively, and the tropical positive and negative precipitation anomaly regions correspond well to the warmer and colder SST regions. Therefore, the above results further suggest that it is the variation of the surface temperature—especially the SST related to ENSO—that apparently induces the adjustments of the SULWRF and precipitation, and then leads to the lower-tropospheric thermal and circulation variations.

Figure 2 shows the latitude–time section of the normalized 1000–500 hPa thickness anomalies averaged over 60°E to 60°W and the Niño3.4 SST anomalies from the developing year [hereafter referred to as (−1)] to the decaying year [hereafter referred to as (0)] of the ENSO events. It can be seen in Figs. 2a and b that the tropical warming (corresponding to the tropical positive thickness anomalies) starts in mid-summer of the developing year of El Niño, lagging the warming of the Niño3.4 SST by about four months. Then, after a short break, the tropical warming strengthens in November (−1) and then reaches its peak in February(0), lagging the peak warming of the Niño3.4 SST by about two months. Thereafter, the tropical warming gradually weakens and ends after the cooling of Niño3.4 SST by one month. Whereas, for La Niña (Figs. 2c and d), the tropical cooling (corresponding to the tropical negative thickness anomalies) starts in April (−1), lagging the cooling of the Niño3.4 SST by one month; and then, the tropical warming strengthens and reaches its peak after the peak cooling of the Niño3.4 SST by about eight months. Thereafter, the tropical cooling continues to the next year of the decaying year. These evolutions of the tropical warming and cooling are consistent with the life cycles of El Niño and La Niña, but their peak time is later than the latter. Another salient feature in Figs. 2a and c is that the extratropical thickness anomalies are in opposite sign with those in tropics, which can also be found in Figs. 1a and e. These results again verify that there are close relations between global circulation and ENSO.

3.2. *Zonal/meridional circulation cycle*

From the above analysis, the global impacts of ENSO can be found not only in the spatial distribution of circulation anomalies during its peak phase, but also in the temporal distribution of circulation anomalies during its evolution. During the peak phase of El Niño, the tropical warming and extratropical cooling enhances the latitudinal temperature gradient. According to the principle of thermal wind adjustment, this results in the strengthening of zonal winds, and in turn leads to the strengthening of zonal circulation. Whereas, during the peak phase of La Niña, the weakened latitudinal temperature gradient results in the weakening of zonal wind, and as a consequence, the zonal circulation weakens while the meridional circulation strengthens. To further check such relationships between the interannual variations of zonal/meridional circulation and the ENSO cycle, three circulation indexes are defined that refer to the distribution of

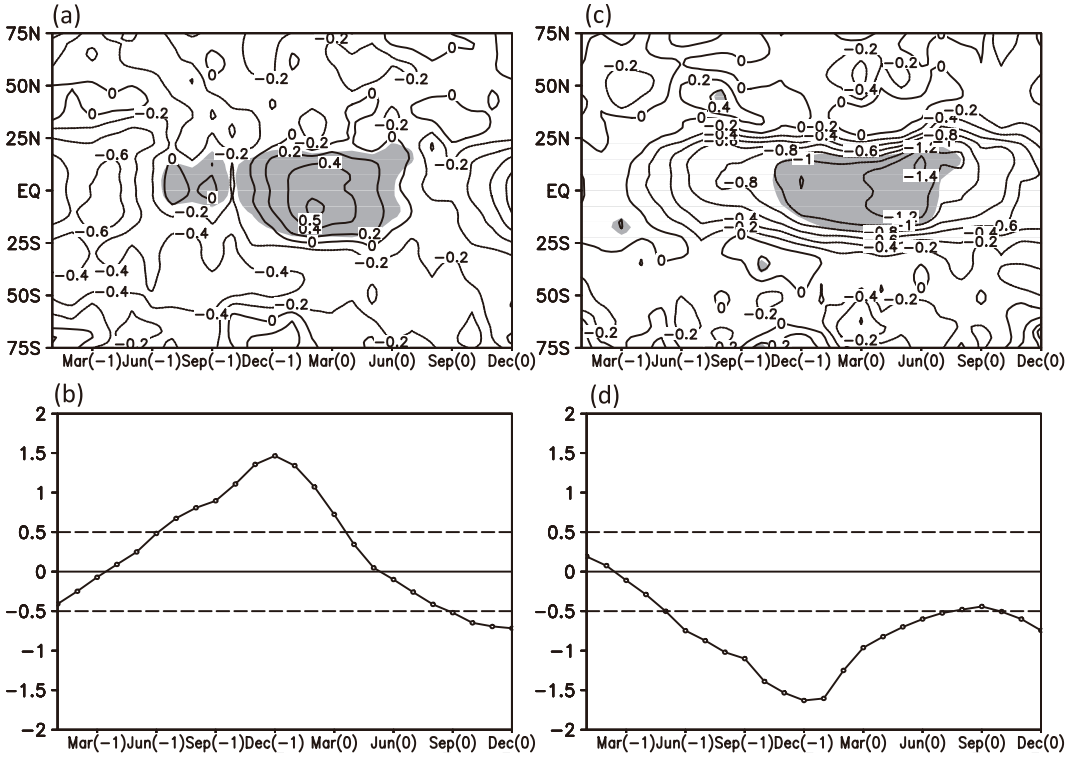

Fig. 2. (a) Latitude–time section of normalized 1000–500 hPa thickness anomalies averaged over 60°E to 60°W (anomalies at the 0.05 significance level are shaded) and (b) Niño3.4 SST anomalies (units: °C) from the developing year(−1) to the decaying year(0) of strong El Niño events. Panels (c) and (d) are the same as (a) and (b), except for La Niña events.

500 hPa geopotential height anomalies during the peak phase of ENSO events (figures omitted). Before the calculation, the linear trend of the 500 hPa geopotential height field was removed.

$$
\begin{aligned}
I_{\mathrm{G}} &= \bar{H}_{(25\mathrm{S}-25\mathrm{N})} - [\bar{H}_{(25\mathrm{S}-50\mathrm{S})} + \bar{H}_{(25\mathrm{N}-50\mathrm{N})}]/2,\\
I_{\mathrm{N}} &= \bar{H}_{(0-25\mathrm{N})} - \bar{H}_{(25\mathrm{N}-50\mathrm{N})},\\
I_{\mathrm{S}} &= \bar{H}_{(0-25\mathrm{S})} - \bar{H}_{(25\mathrm{S}-50\mathrm{S})}.
\end{aligned}
\tag{1}
$$

Here, $I_{\mathrm{G}}, I_{\mathrm{N}}$, and I_{S} are the "global circulation index", the "Northern Hemisphere circulation index", and the "Southern Hemisphere circulation index", respectively. $\bar{H}$ is the mean normalized height anomalies along the latitudinal sector specified in the brackets. Strong positive indexes indicate that the zonal circulation is significant, whereas strong negative indexes suggest that the meridional circulation is prevalent.

Figure 3 depicts the three circulation indexes and the Niño3.4 SST anomalies index in winter, with "E" and "L" corresponding to the peak year of El Niño and La Niña events, respectively. It can be seen that the interannual variations of the three circulation indexes are quite consistent with that of the Niño3.4 SST index. Their correlation coefficients with the Niño3.4 SST index are 0.85 (I_{G}), 0.85 (I_{N}), and 0.89 (I_{S}), respectively, all beyond the 0.001 significance level, implying that zonal and meridional circulation (depicted by the high and low circulation indexes) transit cyclically with a period of 3–5 years, like ENSO. However, this is quite different to the cyclic variation of circulation in the form of the establishment and destruction of zonal circulation, which has a period of just a few weeks (Ye and Zhu, 1958). The former is global, closely related to ENSO and with certain locked flow patterns (Zong et al., 2008), while the latter is triggered by the inner dynamic processes of the atmosphere, at a large scale only, and without a definite flow pattern.

3.3. *Vertical circulations*

Figure 4 shows the zonal mean anomalous vertical circulation, mass streamfunction anomalies and latent heat net flux (LHNF) anomalies during the peak phase of ENSO. During the peak phase of El Niño, three closed circulation cells (Fig. 4a) are located from the low to high latitudes in a clockwise–anticlockwise–clockwise manner in the Northern Hemisphere, but in an anticlockwise–clockwise–anticlockwise manner in the Southern Hemisphere. The mass streamfunction anomaly centers (Fig. 4b) present a similar distribution to these anomalous circulation cells. These results clearly suggest that the Hadley cells (HC), Ferrel cells (FC) and Polar cells (PC) are all strengthened and shift equatorward during the peak phase of El Niño. These results are consistent with previous studies (Seager et al., 2003; Lu et al., 2008). During the peak phase of La Niña, the circulation anomaly cells (Fig. 4c) and mass streamfunction anomalies (Fig. 4d) are generally opposite to those for El Niño (Figs. 4a and b), but located more poleward, suggesting that the HC, FC and PC are weakened and move more poleward.

To elucidate the possible cause of the above variations of vertical circulation, the zonal mean LHNF anomalies are examined. During the peak phase of El Niño, the maximum LHNF anomalies appear where the strongest ascending branches are located; whereas, the minimum LHNF anomalies are situated where the strongest descending branches are located. Similarly, during the peak phase of La Niña, the minimum LHNF anomalies appear near the latitudinal zone of 7°N (Fig. 4f), where the tropical descending branches are located (Fig. 4d). To both sides of this tropical lowest value zone, the LHNF anomalies rise to their peaks near the ascending branches. This indicates that the variation of LHNF in the tropics probably plays a key role in the adjustment of HC, as well as the related circulation and LHNF in the extratropics. Compared with Figs. 4c and f, it shows that the variation of LHNF in the tropics plays a more important role in El Niño than in La Niña events, which is consistent with the work of

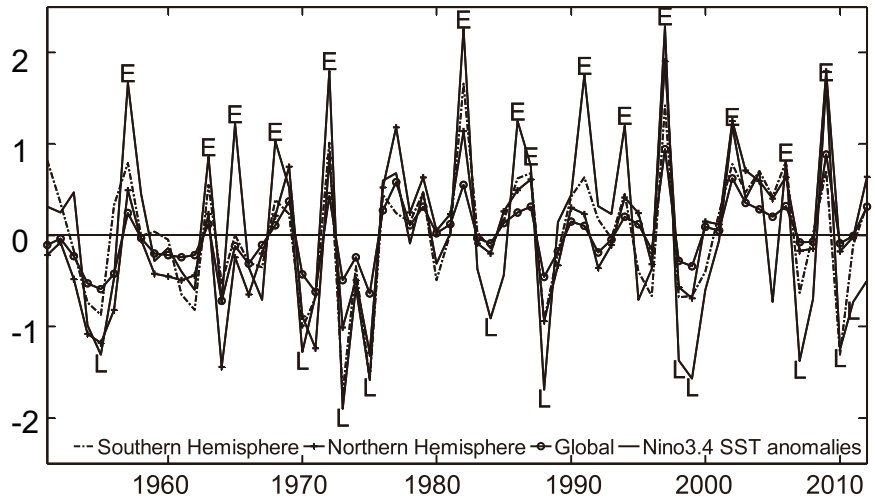

Fig. 3. Time series of three circulation indexes and Niño3.4 winter SST anomalies (units: °C). "E" and "L" refer to the peak year of El Niño and La Niña, respectively.

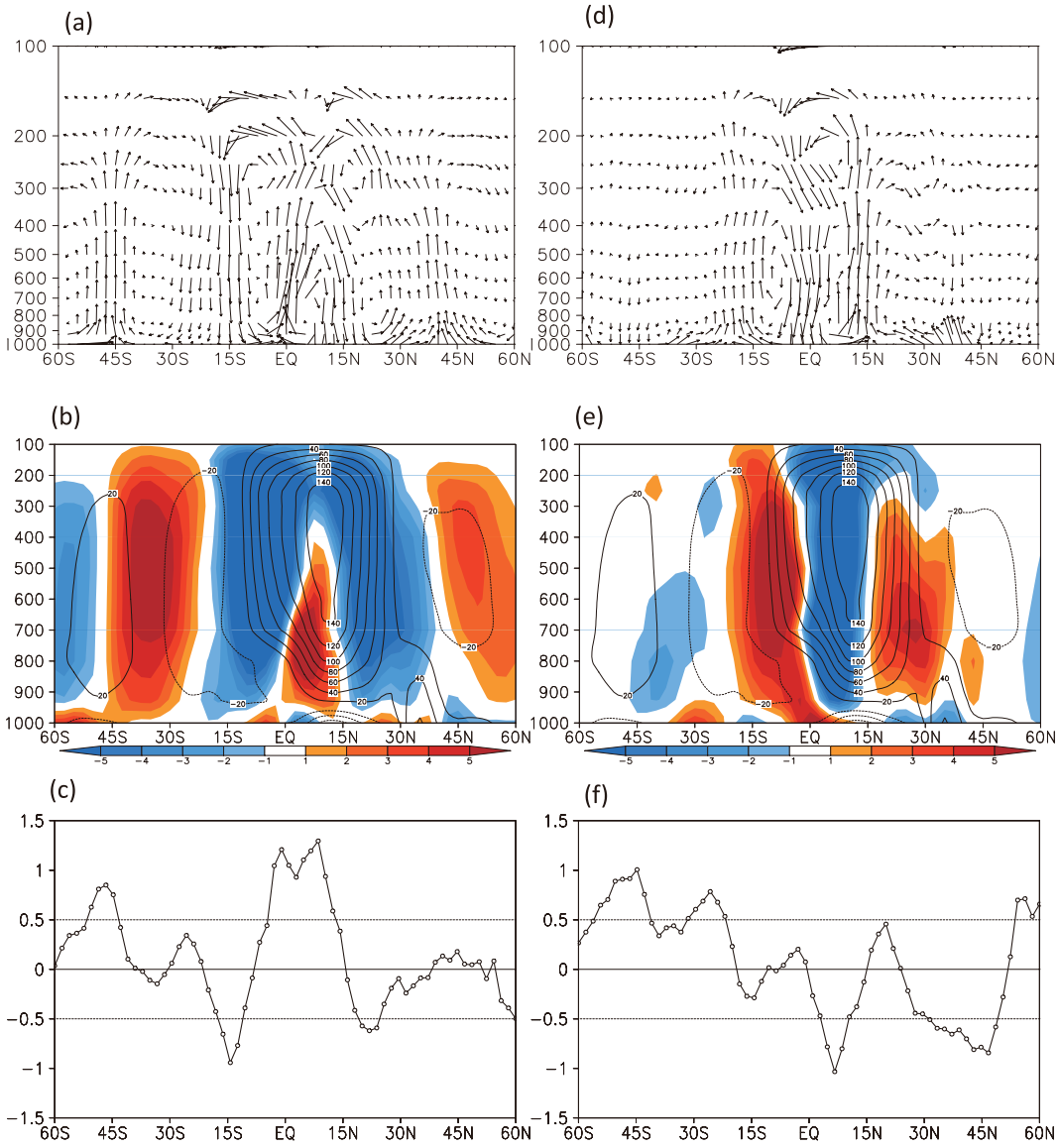

Fig. 4. Zonal mean (a) vertical circulation, (b) mass streamfunction (1×10^9 Kg s^{-1}) and (c) latent heat net flux anomalies (units: W m^{-2}) during the peak phase of El Niño. Panels (d–f) are the same as (a–c), except for during the peak phase of La Niña. Contours in (b) and (e) are the climatological mean mass streamfuction.

Bjerknes (1966, 1969).

Moreover, the impact of ENSO on the Walker circulation (WC) is also profound. During the peak phase of El Niño, the WC becomes weakened and moves eastward as a result of the injection of surplus heat in the central-eastern equatorial Pacific and the lessening of heat supply in the western tropical Pacific (figure omitted). As a result, the convection over the western tropical Pacific is suppressed. This is favorable for the establishment and maintenance of the cross-equatorial anticyclone pair (CEAP) and the equatorial easterly winds in the western tropical Pacific and adjacent areas. Whereas, during the peak phase of La Niña, the WC becomes strengthened as a result of surplus heat supply from the western tropical Pacific and lessening heat supply from the central-eastern equatorial Pacific. This results in enhancement of the convection over the western tropical Pacific and favors the establishment and maintenance of the cross-equatorial cyclone pair (CECP) (Gill, 1980) and the equatorial westerly winds in the western tropical Pacific and adjacent areas.

From all of the above, it can be concluded that the anomalous heat released from the central-eastern equatorial Pacific plays a dominant role in ENSO's driving of global circulation variation, and the HC is a key linkage between ENSO and extratropical circulation. During the peak phase of El Niño, the HC's ascending branch strengthens due to the injection of the tropical heat supply (including longwave-radiation heat and latent heat released by convection). As a result, more tropical surface angular momentum is brought to the upper tropical troposphere by the HC's ascending branch and transported from the tropics to the extratropics via poleward flow and descending branches of HC and FC, resulting in the strengthening of the westerly winds and the prevalence of zonal circula-

tion in the mid-high latitudes of both hemispheres. Whereas, during the peak phase of La Niña, the tropical ascending actions and the poleward flow are weakened for lacking tropical heat supply; the tropical angular momentum transportation from the surface to the upper troposphere, as well as from the tropics to the extratropics, is suppressed, leading to the weakening of the westerly winds and the consequent intensifying of the meridional circulation in the mid-high latitudes. Under the driving force of ENSO, the circulation varies in the form of an alternation between the meridional and zonal circulation at a period of 3–5 years, like the ENSO cycle.

4. Propagating waves of SO/NO and the ENSO cycle

In the 1930s, Walker and Bliss (1932) first reported the Southern Oscillation (SO). In the 1980s, Chen and Zhan (1984) found another zonal oscillation in the tropical North Pacific similar to the SO, and called it the Northern Oscillation (NO). Chen and Fan (1993) and Chen and Wu (2000a, 2000b) found the propagating features of the sea level pressure (SLP) anomalies associated with the SO/NO using ten years of data, and pointed out that these anomalies can be tracked back to the mid-high latitudes. In this section, we further study the propagating waves of SO/NO and their link with the ENSO cycle using longer period datasets.

4.1. *Features of the propagating waves of SO/NO and SST*

Figure 5 presents the lagging regression maps of 850 hPa wind anomalies, SST anomalies and precipitation anomalies along the equator (averaged over 5°S–5°N) against the Niño3.4 winter SST from winter (−2) to summer (1) over four years. Here, (−2) and (−1) refer to two years and one year before the Niño3.4 winter SST, respectively, while (0) and (1) refer to the same year and one year after the Niño3.4 winter SST, respectively.

In winter (−2) (Fig. 5a), the EAWM and the Australian summer monsoon (ASM) are stronger than normal. Two anomalous cyclones dominate over the western North Pacific and west of Australia, respectively, forming a cyclone pair crossing the equator; namely, the CECP (Chen and Wu, 2000a). Anomalous westerly winds prevail along the equator between the two anomalous cyclones. A CEAP is located over the eastern Pacific, with anomalous easterly winds prevailing over the central-eastern equatorial Pacific. The SST anomalies are negative in the central-eastern equatorial Pacific and positive near the warm pool region, similar to the distribution of SST anomalies during the peak phase of La Niña. Such a distribution indicates that the SO/NO and ENSO are both in the peak phase of La Niña. The appearance of anomalous westerly winds over the western equatorial Pacific provides one of the conditions for La Niña decay and the occurrence of an El Niño (Huang and Fu, 1996; Li and Mu, 1998; Bueh and Ji, 1999).

In summer (−2) (Fig. 5b), the western Pacific CECP expands eastward to east of the dateline. The anomalous westerly winds over the western equatorial Pacific also shift eastward. At the same time, the eastern Pacific CEAP shifts poleward and retreats westward, resulting in the weakening of trade wind anomalies in the central-eastern equatorial Pacific. These features of wind anomalies imply that the SO/NO indexes are weakening. The weakened negative SST anomalies in the central-eastern equatorial Pacific indicate that the La Niña is decaying.

In winter (−1) (Fig. 5c), with the farther-eastward shifting and expansion of the western Pacific CECP, the anomalous westerly winds over the western equatorial Pacific propagate eastward to 170°E, the eastern Pacific CEAP shifts poleward, and the anomalous easterly winds over the central-eastern equatorial Pacific weaken. The SST anomalies in most parts of the central-eastern equatorial Pacific have risen above −0.3°C. The SO/NO cycle and the ENSO cycle are all in their neutral phase from La Niña to El Niño.

In summer (−1) (Fig. 5d), the CECP has shifted to the eastern Pacific and the tropical Pacific is dominated by the anomalous westerly winds. Meanwhile, a newly forming CEAP replaces the CECP over the western Pacific. The negative central-eastern equatorial Pacific SST anomalies have changed into positive ones with maximum values exceeding 0.9°C, indicating that the SO/NO have changed into their negative phase and El Niño occurs.

In winter (0) (Fig. 5e), the distributions of the wind and SST anomalies are more like those in winter (−2) (Fig. 5a), but opposite in sign. The EAWM and ASM are weaker. The CEAP dominates over the western Pacific and eastern Indian Ocean, accompanied by prevailing easterly wind anomalies between the CEAP. At the same time, the CECP over the eastern Pacific maintains the enhancement of westerly wind anomalies and the strengthening of positive central-eastern equatorial Pacific SST anomalies. This distribution of CEAP and CECP indicates that the SO/NO are in strong negative phases and the distribution of SST anomalies implies that the El Niño has been in its peak.

In summer (0) (Fig. 5f), the CEAP expands eastward to east of 180°E and the eastern Pacific CECP weakens and shifts poleward with the eastward propagation of easterly wind anomalies over the western tropical Pacific and the weakening of central-eastern equatorial Pacific westerly wind anomalies. This implies that the SO/NO are decaying from their strong negative phases; and the weakened positive central-eastern equatorial Pacific SST anomalies show that the El Niño is decaying from its peak phase.

In winter (1) (Fig. 5g), with the main centers of CEAP shifting to the east of 180°E, the easterly wind anomalies have propagated to the eastern equatorial Pacific, implying that the SO/NO have changed to positive phase again. The reoccurrence of the negative central-eastern equatorial Pacific SST anomalies indicates that the ENSO cycle is in the neutral phase from El Niño to La Niña.

In summer (1) (Fig. 5h), a new CECP appears over the eastern Indian Ocean–western Pacific, with the prevalence of anomalous westerly winds over the tropical Indian Ocean and the east part of the Maritime Continent. The CEAP shifts to the eastern Pacific with the strengthening of easterly winds

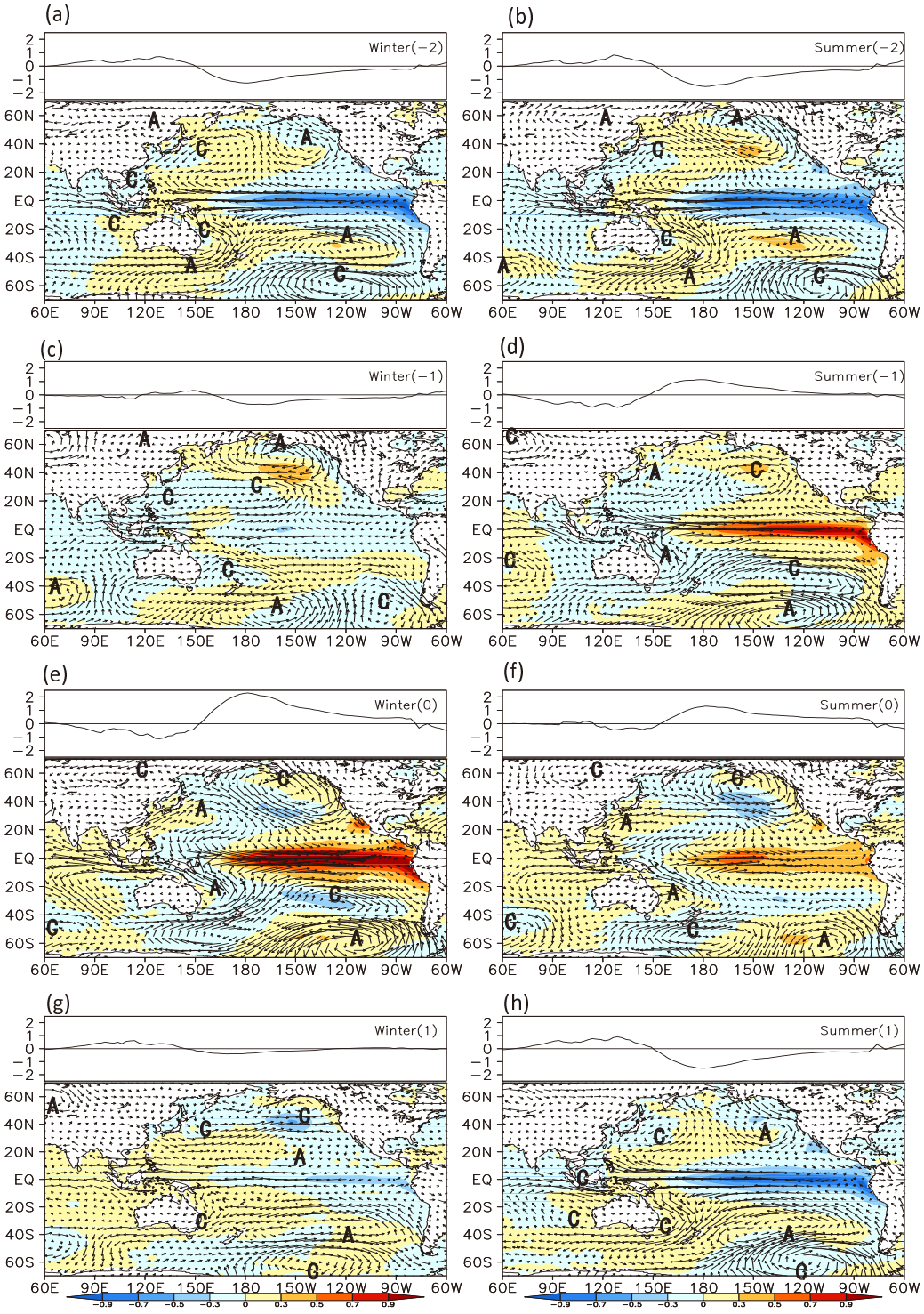

Fig. 5. Lagging regression maps of 850 hPa winds anomalies (vectors; units: m s^{-1}), SST anomalies (shading; units: °C), and precipitation anomaly (line; units: mm) along the equator (averaged over 5°S–5°N) against the Niño3.4 winter SST anomalies from (a) winter (−2) to (h) summer (1).

over the central-eastern equatorial Pacific. This indicates that SO/NO are stronger than normal. The strengthening of the negative SST anomalies indicates the development of La Niña.

The above results show that the characteristic pattern of SO/NO is not a standing seesaw, but consists of the process of eastward propagation of SLP anomalies along the subtropical Pacific. With the eastward propagation of SLP anomalies, the whole ENSO cycle takes about 4 years from La Niña to El Niño and again from El Niño to La Niña, mainly consisting of eight phases: the developing, peak, and decaying phases of La Niña and El Niño, and the neutral phases from

La Niña to El Niño and from El Niño to La Niña. Zong and Chen (2013) found that different phases of the ENSO cycle have different influences on the long-term synoptic processes of intraseasonal variation of the summer monsoon rain belt over eastern China.

4.2. *Interactions between the propagating waves of SO/NO and the ENSO cycle*

Figure 5 also shows that the formation of the ENSO cycle is closely related to the evolutions of the anomaly centers of SO/NO. The meridional flow pattern forced by La Niña initiates stronger EAWM and ASM, resulting in the formation and strengthening of the anomalous CECP (anomaly centers of SO/NO in the eastern hemisphere) and the strengthening of convections near the Philippine Islands and the eastern Indian Ocean (Figs. 5a and b). With the expansion and shifting of the CECP to the central tropical Pacific (Fig. 5c), the western Pacific westerly wind anomalies expand eastward, leading the central-eastern equatorial Pacific SST into a neutral phase of the ENSO cycle. The convections in the western equatorial Pacific are weakened. When the CECP moves to the eastern Pacific and a new CEAP appears in the western Pacific (Fig. 5e), the SO/NO shift into their negative phases, and the anomalous westerly winds cover the whole central-eastern equatorial Pacific and reach their maximum amplitudes. At the same time, the SST anomalies and convections in the central-eastern equatorial Pacific reach their maximum amplitudes, suggesting a change into the peak phase of El Niño. Thereafter, as a consequence of the strengthening of convection and heat release in the central-eastern equatorial Pacific triggered by El Niño, the HC becomes strengthened, resulting in the prevalence of zonal circulation in the mid-high latitudes. Consequently, the EAWM and ASM become weakened, resulting in the formation and strengthening of CEAP and a weakening of convections near the western equatorial Pacific. With the expansion and shifting of the CEAP to the central Pacific (Fig. 5g), the anomalous easterly winds in the western Pacific expand eastward, leading the central-eastern equatorial Pacific SST into a neutral phase of the ENSO cycle again. When the CEAP moves to the eastern Pacific and a new CECP appears in the western Pacific, as depicted in Fig. 5a, the SO/NO shift into their positive phases and the ENSO cycle shifts into the peak phase of La Niña again. A complete ENSO cycle is thus complete. It suggests that the eastward propagation of the anomaly centers of SO/NO plays a key role in linking among the flow patterns in the mid-high latitudes forced by ENSO, the Asian and Australian monsoons, the equatorial Pacific wind and SST, and ENSO events.

On the other hand, the variation of the central-eastern equatorial Pacific SST plays a dominant role in the eastward propagation of the anomaly centers of SO/NO. In the peak phase of La Niña (Fig. 5a), the equatorial Pacific SST anomalies reach their maximum amplitudes; at the same time, associated with the strengthening of the CECP over the Philippine Islands and the eastern Indian Ocean, another CECP is strengthening west of the dateline, where the subtropical high is located, acting like the strengthening of the CECP over the Philippine Islands and the eastern Indian Ocean. This suggests that these changes of the western Pacific CECPs are interconnected with the anomalous heating of the equatorial Pacific through the HC and WC. The decreased heating in association with La Niña induces the weak HC and the strong WC. The CECP west of the dateline, in association with La Niña, is located exactly in the sinking region of the HC. Therefore, the weak HC favors the development of CECP over that region. Meanwhile, during the peak phase of La Niña, both the WCs over the equatorial Indian and Pacific oceans are strengthened with their ascending branches over the western Pacific warm pool region, favoring the development of CECP over the Philippine Islands and the eastern Indian Ocean. In the decaying phase of La Niña (Fig. 5b), with the eastward shift of the ascending branch, the anomalous westerly winds over the western equatorial Pacific also shift eastward. The CECP west of the dateline extends eastward due to the lagging heating of the SST anomaly. In the transition phase from La Niña to El Niño (Fig. 5c), the CECP west of the dateline moves to near the dateline and the CECP over the Philippine Islands and the eastern Indian Ocean weakens and disappears. During the developing and peak phase of El Niño (Figs. 5d and e), as a consequence of the strengthening of convections and positive SST anomalies in the central-eastern equatorial Pacific, the HC strengthens while the WC weakens, resulting in the shifting of CECP to the eastern Pacific and the formation and strengthening of CEAP in the western Pacific. In the decaying phase of El Niño (Fig. 5f), with the eastward shift of the descending branch, the anomalous easterly winds over the western equatorial Pacific also shift eastward. The CEAP extends eastward near the dateline due to the lagging heating of the SST anomaly. In the transition phase from El Niño to La Niña(Fig. 5g), the CEAP moves to east of the dateline and the CEAP in the western Pacific disappears. In the developing phase of La Niña (Fig. 5h), associated with the weakening of convection and decreasing of SST in the central-eastern equatorial Pacific, the HC weakens while the WC strengthens, resulting in the formation and strengthening of CECP over the western equatorial Pacific and eastern tropical Indian Ocean. Therefore, the eastward propagations of the positive and negative SLP anomalies of SO/NO are closely interconnected with the evolutions of the HC and WC resulting from the adjustment of heating in the central-eastern equatorial Pacific, and present a cycle over a period of 3–5 years, similar to that of the ENSO cycle. Here, the role of SST in the central-eastern equatorial Pacific is highlighted. However, it should be mentioned that the extratropical air–sea interactions are also very important for the eastward propagations of the anomaly centers, but detailed discussion on this topic is beyond the scope of the present paper.

The above analysis verifies the propagating waves of SO/NO reported by Chen and Fan (1993) using a longer dataset. Moreover, it further depicts the feedbacks between the tropical and extratropical anomalous circulation and ENSO. The propagating waves of SO/NO play an important connect-

ing role in the feedback processes between the anomalous circulation and ENSO; for instance, the transition between the anomalous meridional and zonal flow pattern, anomalous westerly and easterly winds, El Niño and La Niña events, as well as the transition between strong and weak EAWM, HC and WC.

5. Discussion and summary

Using longer datasets than in previous research, we examined the spatiotemporal distributions of global thermal and circulation anomalies associated with ENSO and the possible contributions of the HC, WC and propagating waves of SO/NO to the formation of the ENSO cycle. The results indicate that the anomalous convection and heat release triggered by the central-eastern equatorial Pacific SST anomalies is the primary factor driving the 3–5 year cycle of ENSO. The enhanced heating associated with El Niño induces the enhancement of HC and latitudinal temperature gradient and the weakening of WC. The former two favor the development of zonal circulation in the mid-high latitudes through stronger zonal angular momentum transport from the tropics to the extratropics and thermal wind adjustment, respectively, while the latter favors the appearance of anomalous easterly winds east to its anomalous descending branch in the western equatorial Pacific. On the contrary, the HC and latitudinal temperature gradient are weakened and the WC is strengthened in association with the decreased heating triggered by La Niña. As a result, the zonal winds in mid-high latitudes are weakened due to the lessening of zonal angular momentum transport by HC from the tropics to the extratropics and thermal wind adjustment induced by the decreased latitudinal temperature gradient, which in turn favors the intensification of meridional circulation in the midlatitudes. Therefore, the HC and WC play a key role in the linking of ENSO with the circulations in the mid-high latitudes and the zonal winds in the equatorial Indian and Pacific oceans.

Forced by ENSO, the circulation in the mid-high latitudes alternates between anomalous meridional and zonal circulation patterns with a period of 3–5 years. This differs to the circulation variation triggered by the inner dynamic processes of the atmosphere, which occurs over a period of about several weeks and without a definite flow pattern.

The anomalous zonal flow pattern triggered by El Niño results in weaker EAWM/ASM and WC, and in turn leads to the development of the CEAP and occurrence of anomalous easterly winds over the western equatorial Pacific, providing one of the essential conditions for the occurrence of the next La Niña. Whereas, the anomalous meridional flow pattern triggered by La Niña results in stronger EAWM/ASM and WC, and in turn leads to the development of the CECP and occurrence of anomalous westerly winds over the western equatorial Pacific, providing one of the essential conditions for the occurrence of the next El Niño.

The CEAP and CECP are actually a component part of SO/NO. The characteristic pattern of the SO/NO is not a standing seesaw, but consists of the process of eastward propagation of anomaly centers along the subtropical Pacific due to the evolution of the HC and WC. The enhanced HC induces the development of the positive SLP anomalies over the subtropical Pacific near the dateline while the gradual strengthening of WC induces the decaying of the positive SLP anomalies over the southwestern and northwestern Pacific, leading to the eastward shifting of CEAP and anomalous easterly winds from the western to the central Pacific. These eastward propagations lead to the decreasing of SST in the central-eastern equatorial Pacific and the ultimate occurrence of La Niña through air–sea interaction. Whereas, the decreased HC and gradual weakening of WC lead to the east-

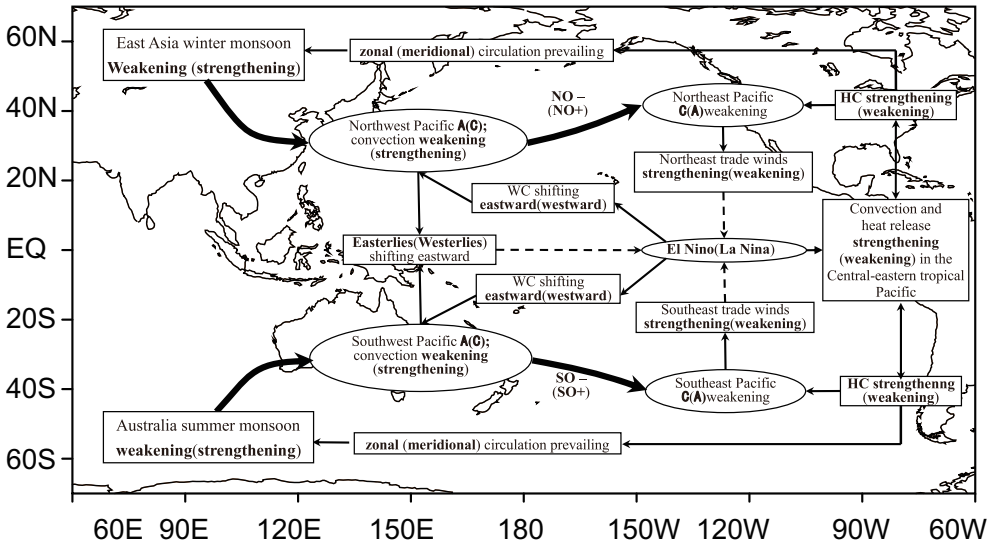

Fig. 6. Schematic diagram of the physical model for the formation of the ENSO cycle. "**A**" and "**C**" refer to anticyclone and cyclone, respectively. Solid (dashed) arrows indicate positive (negative) feedback processes.

ward propagation of CECP and anomalous westerly winds from the western to the eastern Pacific, resulting in the increasing of SST in the central-eastern equatorial Pacific and the occurrence of El Niño. In the above processes, the propagating waves of SO/NO play an important connecting role between the extratropical circulation and the central-eastern equatorial Pacific SST.

The physical model of the formation of the ENSO cycle is mainly composed of two fundamental processes at the basin scale and global scale, respectively. The basin-scale process is the outcome of air–sea interactions in the central-eastern equatorial Pacific (Fig. 6, right). During the peak phase of El Niño (La Niña), the SO/NO exhibit a distribution with anomalous cyclones (anticyclones) in the eastern Pacific and anomalous anticyclones (cyclones) in the western Pacific. The stronger (weaker) convection and heat release lead to the weakening (strengthening) of the anomalous cyclone in the southeastern and northeastern Pacific through the HC. In turn, the southeast and northeast trade winds strengthen (weaken), and the advection and upwelling of cold water strengthens (weakens) in the central-eastern equatorial Pacific, resulting in the decreasing (increasing) of SST there. This negative feedback process results in the occurrence of a La Niña (El Niño) and ultimately fulfills the ENSO cycle. The global-scale process involves the contribution of extratropical circulation anomalies (Fig. 6, left). During the peak phase of El Niño (La Niña), the enhanced (decreased) heating in the central-eastern equatorial Pacific induces the prevalence of the zonal (meridional) flow pattern in the midlatitudes in both hemispheres through the stronger (weaker) HC, then leads to the weaker (stronger) EAWM and ASM, which favors the formation and eastward shift of the CEAP (CECP) and the easterly (westerly) wind anomalies. Through this negative feedback process, La Niña (El Niño) ultimately appears and completes the transition from El Niño to La Niña (La Niña to El Niño). Therefore, the ENSO cycle, at the basin scale, has a direct impact on the lower-tropospheric wind over the central-eastern equatorial Pacific; whereas at the global scale, it has a decisive influence on lower-tropospheric wind over the western tropical Pacific.

This paper mainly demonstrates the processes involved in the formation of an average ENSO cycle and its interactions with the propagating waves of SO/NO. However, for a specific ENSO cycle, its intensity and persistence time will differ. Moreover, the ENSO cycle can be classed into two types according to the location of the warming: the central-Pacific-type and eastern-Pacific-type (Kao and Yu, 2009, Sun et al., 2013; Xu et al., 2013). Jin and Chen (1992) pointed out that if the SO changes into its negative phase earlier than the NO, warming usually appears in the southeastern Pacific first, and an eastern-Pacific-type El Niño occurs; whereas, when the NO changes into its negative phase earlier than the SO, warming usually appears in the central Pacific first, and a central-Pacific-type El Niño occurs. However, at present, the physical processes underlying the two El Niño types are yet to be completely revealed and understood, and further studies are still needed.

Acknowledgements. The author thanks Professor CHEN Lieting and Professor JI Liren for their help in revising the paper. This work was jointly supported by the National Natural Science Foundation of China (Grant No. 41375055), the National Basic Research Program of China (Grant No. 2012CB957804), the Key Technologies R&D Program (Grant No. 2009BAC51B02), and the State Grid Science & Technology Project (GC71-13-007).

REFERENCES

Battisti, D. S., and A. C. Hirst, 1989: Interannual variability in the tropical atmosphere ocean system: Influence of the basic state and ocean geometry. *J. Atmos. Sci.*, **46**, 1687–1712.

Bjerknes, J., 1966: A possible response of the atmospheric hadley circulation to equatorial anomalies of ocean temperature. *Tellus*, **18**, 820–829.

Bjerknes, J., 1969: Atmospheric teleconnections from the equatorial Pacific. *Mon. Wea. Rev.*, **97**, 163–172.

Bueh, C., and L. R. Ji, 1999: Abnormal East Asia winter monsoon and tropical Pacific SST anomalies. *Chinese Science Bulletin*, **44**, 252–259. (in Chinese)

Cane, M. A., and S. E. Zebiak, 1985: A theory for El Niño and the Southern Oscillation. *Science*, **228**, 1085–1087.

Chao, J. P., and R. H. Zhang, 1988: The air-sea interaction waves in the tropics and their instabilities. *Acta Meteorologica Sinica*, **2**, 275–287.

Chen, D., and M. A. Cane, 2008: El Niño prediction and predictability. *J. Comput. Phys.*, **227**, 3625–3640.

Chen, L. T., 1982: Interaction between the subtropical high over the North Pacific and the sea surface temperature of the eastern equatorial Pacific. *Scientia Atmospherica Sinica*, **6**, 148–156. (in Chinese)

Chen, L. T., and Z. Q. Zhan, 1984: Teleconnection of pressure anomaly between the east and west of the northern Pacific. *Chinese Science Bulletin*, **29**, 481–483. (in Chinese)

Chen, L. T., and Z. Fan, 1993: The southern oscillation/northern oscillation cycle associated with sea surface temperature in the equatorial Pacific. *Adv. Atmos. Sci.*, **10**, 353–364.

Chen, L. T., and R. G. Wu, 2000a: The role of the Asian/Australian monsoons and the Southern/Northern oscillation in the ENSO cycle. *Theor. Appl. Climatol.*, **65**, 37–47.

Chen, L. T., and R. G. Wu, 2000b: ENSO cycle associated with Asian/Australian monsoon and Southern/Northern Oscillation. *Acta Meteorologica Sinica*, **58**, 168–178. (in Chinese)

Fu, Y. F., and R. H. Huang, 1996: The effect of the westerly anomalies over the tropical Pacific on the occurrence of ENSO events. *Scientia Atmospherica Sinica*, **20**, 641–654. (in Chinese)

Gill, A. E., 1980: Some simple solutions for heat-induced tropical circulation. *Quart. J. Roy. Meteor. Soc.*, **106**, 447–662.

Hirst, A. C., 1988: Slow instabilities in tropical ocean basin–global atmosphere models. *J. Atmos. Sci.*, **45**, 830–852.

Huang, R. H., and Y. F. Fu, 1996: Some progresses and problems in the study on the dynamics of the ENSO cycle. *Disastrous Climate*, R. Huang, L. Chen, X. Weng, and Z. Song, Eds., China Meteorological Press, 172–188. (in Chinese)

Jin, Z. H., and L. T. Chen, 1992: Contrastion relations between northern and southern with Pacific SST. *Acta Oceanologica Sinica*, **14**, 19–27. (in Chinese)

Kalnay, E., and Coauthors, 1996: The NCEP/NCAR 40-year reanalysis project. *Bull. Amer. Meteor. Soc.*, **77**, 437–471.

Kao, H.-Y., and J.-Y. Yu, 2009: Contrasting eastern-Pacific and central-Pacific types of ENSO. *J. Climate*, **22**, 615–632.

Keen, R. A., 1982: The role of cross-equatorial tropical cyclone pairs in the southern oscillation. *Mon. Wea. Rev.*, **110**, 1405–1416.

Li, C. Y., 1988: Frequent actions of strong East Asian trough and occurrence of El Niño events. *Science in China*, **32**, 667–674. (in Chinese)

Li, C. Y., and M. Q. Mu, 1998: Numerical simulations of anomalous winter monsoon in East Asia exciting ENSO. *Scientia Atmospherica Sinica*, **22**, 481–490. (in Chinese)

Li, Y., X. Q. Yang, and Q. Xie, 2010: Selective interaction between interannual variability of North Pacific subtropical high and ENSO cycle. *Chinese Journal of Geophysics*, **53**, 1543–1553. (in Chinese)

Lu, J., G. Chen, and D. M. W. Frierson, 2008: Response of the Zonal Mean Atmospheric Circulation to El Niño versus Global Warming. *J. Climate*, 21, 5835–5851.

McCreary, J., and P. Julian, 1983: A model of tropical ocean-atmosphere interaction. *Mon. Wea. Rev.*, **111**, 370–387.

Nitta, T., 1989: Global features of the Pacific-Japan Oscillation. *Meteor. Atmos. Phys.*, **41**, 5–12.

Philander, S. G. H., T. Yamagata, and R. C. Pacanowski, 1984: Unstable air-sea interactions in the tropics. *J. Atmos. Sci.*, **41**, 604–613.

Rasmusson, E. M., and T. H. Carpenter, 1982: Variations in tropical sea surface temperature and surface wind fields associated with the Southern Oscillation/El Niño. *Mon. Wea. Rev.*, **110**, 354–384.

Schopf, P. S., and M. J. Suarez, 1988: Vacillations in a coupled ocean–atmosphere model. *J. Atmos. Sci.*, **45**, 549–566.

Seager, R., N. Harnik, Y. Kushnir, W. Robinson, and J. Miller, 2003: Mechanisms of hemispherically symmetric climate variability. *J. Climate*, 16, 2960–2978.

Smith, T. M., R. W. Reynolds, T. C. Peterson, and J. Lawrimore, 2008: Improvements to NOAA's historical merged land–ocean surface temperature analysis (1880–2006). *J. Climate*, **21**, 2283–2296.

Suarez, M. J., and P. S. Schopf, 1988: A delayed action oscillator for ENSO. *J. Atmos. Sci.*, **45**, 3283–3287.

Sun, D., F. Xue, and T. J. Zhou, 2013: Impacts of two types of El Niño on atmospheric circulation in the Southern Hemisphere. *Adv. Atmos. Sci.*, **30**, 1732–1742, doi: 10.1007/s00376-013-2287-9.

Tang, Y., 2002: Hybrid coupled models of the tropical Pacific: I. Interannual variability. *Climate Dyn.*, **19**, 331–342.

Walker, G. T., and E. W. Bliss, 1932: World weather V. *Mem. Roy. Meteor. Soc.*, **4**, 53–84.

Wang, Z. G., R. N. Xing, and X. R. Chen, 2004: Relationship of El Niño with the anomalous westerly wind over equatorial Pacific. *Chinese J. Atmos. Sci.*, **28**, 441–454. (in Chinese)

Wu, A., W. W. Hsieh, and B. Tang, 2006: Neural network forecasts of the tropical Pacific sea surface temperatures. *Neural Networks : The Official Journal of the International Neural Network Society*, **19**, 145–154.

Wu, R. G., and L. T. Chen, 1995: 3-5 year time scale evolution of global 1000 hPa height anomaly during 1980-1989. *Scientia Atmospherica Sinica*, **19**, 575–585. (in Chinese)

Wu, R. G., J. L. Chen, and W. Chen, 2012: Different types of ENSO influences on the Indian summer monsoon variability. *J. Climate*, **25**, 903–920.

Wyrtki, K., 1975: El Niño-the dynamic response of the equatorial Pacific ocean to atmospheric forcing. *J. Phys. Oceanogr.*, **5**, 572–584

Xie, S.-P., Q. Xie, D. Wang, and W. T. Liu, 2003: Summer upwelling in the South China Sea and its role in regional climate variations. *J. Geophy. Res.*, **108**(C8), doi: 10.1029/2003JC001867.

Xu, K., C. W. Zhu, and J. H. He, 2013: Two types of El Niño-related Southern Oscillation and their different impacts on global Land precipitation. *Adv. Atmos. Sci.*, **30**, 1743–1757, doi: 10.1007/s00376-013-2272-3

Ye, D. Z., and B. Z. Zhu, 1958: *Some Basic Problems of Atmospheric Circulation*. Science Press, 159 pp. (in Chinese)

Yun, K.-S., K.-H. Seo, and K.-J. Ha, 2008: Relationship between ENSO and northward propagating intraseasonal oscillation in the east Asian summer monsoon system. *J. Geophys. Res.*, **113**(D14), doi: 10.1029/2008JD009901.

Zhang, R. H., and J. P. Chao, 1993: Unstable tropical air-sea interaction waves and their physical mechanisms. *Adv. Atmos. Sci.*, **10**, 61–70.

Zhang, Z. Q., Y. H. Ding, and Z. C. Zhao, 2000: On the westerly wind outbursts in equatorial western Pacific during the onset and development phases of ENSO and before. *Acta Meteorologica Sinica*, **58**, 11–25. (in Chinese)

Zhu, J. S., G.-Q. Zhou, R.-H. Zhang, and Z. B. Sun, 2013: Improving ENSO prediction in a hybrid coupled model with an embedded entrainment temperature parameterisation. *Inter. J. Climatol.*, **33**, 343–355.

Zong, H. F., and L. T. Chen, 2013: Characteristics of the atmospheric circulation and sea surface temperature for different modes of intraseasonal variation of summer monsoon rain belt in eastern China. *Chinese J. Atmos. Sci.*, **37**, 1072–1082. (in Chinese)

Zong, H. F., Q. Y. Zhang, and L. T. Chen, 2008: A study of the processes of East Asia-Pacific teleconnection pattern formation and the relationship to ENSO. *Chinese J. Atmos. Sci.*, **32**, 220–230. (in Chinese)